Journal Name

ARTICLE TYPE

Cite this: DOI: 10.1039/xxxxxxxxxx

Supplementrary Information: When does near-wall hindered diffusion influence mass transport towards targets?

Shaltiel Eloul[a],Enno Kätelhön[a], and Richard G. Compton*[a]

1 Computational methods

Numerical calculations of the non-homogeneous and anisotropic diffusion equations were carried out using the Implicit Finite difference method for 1D cases and combined with the ADI method for the 2D anisotropic case. The Thomas algorithm was employed to solve the discrete concentration equations[1,2]. For the 2D parametric study, which contains thousands of runs for each case, we implemented a GPU high-performance solver using the implicit parallel algorithm for voltammetry[3].

The mesh was created using an expanding grid to provide sufficiently small differences next to the walls and the target surface. The near-wall hindered diffusion problem is very sensitive to meshing and the convergence of the result varies for different sizes of particles due to the diffusion coefficient profile close to the wall. Therefore, a careful convergence test was carried out to evaluate the minimum difference ($10^{-7} \cdot r_s$) and the expansion factors (1.06 in both r and z directions) required for achieving an accurate simulation in the near-wall hindered diffusion simulation for $r_p > 5$nm.

1.1 Accuracy and convergence tests

Initial tests were carried out using non-hindered cases to provide a full agreement (within 0.6 % for all time) of the mass balance equations with theoretical transient flux towards the disc and a sphere[4]. The expansion factor parameter, the minimum difference, and the tunnelling rate coefficient (ν) for the non-hindered case were varied until the result for the flux converged to the value for the simplified model of no-tunnelling but fully adsorbing surface. In the parametric study, which contains 4000 runs to find the steady state, a global convergence approach was used as follows: The simulation was run and then fitted to the function to find the coefficients (Eq. **??**, **??**). Thereafter, the mesh parameters were varied until the coefficients of the fitted equation remained constants.

1.2 Implementation

All simulations were implemented using C++. For the parametric study, the parallelization of ADI solver was implemented using NVIDIA CUDA. The processor was a Xeon E5-1650, 3.2GHz, and 16GB of RAM. The GPU is a NVIDIA Quadro K4000 (Kepler architecture). Least squares fittings using the 'general-model' fit function as well as post-processing procedures were carried out in Matlab software.

* *Corresponding Author.*
[a] *Department of Chemistry, Physical and Theoretical Chemistry, Oxford University, South Parks Road, Oxford OX1 3QZ, United Kingdom.*

2 Diffusion to a finite sphere

2.1 Non-hindered diffusion case

The solution of diffusion towards a sphere or an hemi-sphere can be found through solving the diffusion equation in one dimensional radial coordinates system:

$$\frac{\partial c}{\partial t} = D(\frac{\partial^2 c}{\partial r^2} + \frac{2}{r}\frac{\partial c}{\partial r}) \tag{1}$$

with boundary conditions of a full adsorbing surface on the sphere with a radius r_s, and bulk concentration is assumed at infinite distance:

$$t \geq 0, \quad r = r_s, \quad c = 0 \tag{2}$$

$$t \geq 0, \quad r = \infty, \quad c = c^* \tag{3}$$

Changing the variable:

$$u = -cr \tag{4}$$

gives the equation

$$\frac{\partial u}{\partial t} = D(\frac{1}{r}\frac{d^2 u}{dr^2}) \tag{5}$$

It requires the introduce of a new variable:

$$\eta = \frac{r}{2\sqrt{Dt}} \tag{6}$$

and the diffusion equation becomes:

$$\frac{d^2 u}{d\eta^2} + 2\eta\frac{du}{d\eta} = 0 \tag{7}$$

This gives the solution to be of the form:

$$\frac{du}{d\eta} = ae^{-\eta^2} \tag{8}$$

Integrating and applying the bulk boundary condition at infinity gives:

$$\int_u^{u^*} du = a\int_\eta^\infty e^{-\eta^2} d\eta \tag{9}$$

$$u^* - u = a(\frac{\sqrt{\pi}}{2} - e^{-\eta^2} d\eta) \tag{10}$$

Using the boundary condition of a fully adsorbing surface at $r = r_s$, we get:

$$a = -(\frac{2}{\sqrt{\pi}})rc^* \tag{11}$$

and substituting back:

$$c = c^*\{1 - \frac{r_s}{r}(1 - erf(\frac{r - r_s}{\sqrt{4Dt}})\} \tag{12}$$

$$c = c^*\{1 - \frac{r_s}{r}(1 - \frac{2}{\sqrt{\pi}}\sum_0^\infty \frac{(-1)^n z^{2n+1}}{n!(2n+1)})\} \text{ where } z = \frac{r - r_c}{\sqrt{4Dt}} \tag{13}$$

Finding the flux:

$$D\frac{dc}{dr}|_{r=r_s} = Dc^*\{\frac{r_c}{r}\frac{2}{\sqrt{\pi}}(\sum_0^\infty \frac{(-1)^n z^{2n}}{n!}\frac{dz}{dr}) + \frac{r_s}{r^2}(1 - \frac{2}{\sqrt{\pi}}\sum_0^\infty \frac{(-1)^n z^{2n+1}}{n!(2n+1)})\} \tag{14}$$

where

$$z = \frac{r - r_s}{\sqrt{4Dt}}, \quad \frac{dz}{dr} = \frac{1}{\sqrt{4Dt}} \tag{15}$$

Expanding the Taylor series:

$$D\frac{dc}{dr}|_{r=r_s} = Dc^*\{\frac{2}{\sqrt{\pi}}(1 - z^2 + \frac{z^4}{2} - ...)(\frac{1}{\sqrt{4Dt}}) + \frac{2}{\sqrt{\pi}}(-z + \frac{z^3}{3} - ...) + \frac{1}{r_s})\} \tag{16}$$

Since $z = \frac{r - r_s}{\sqrt{4Dt}} = 0$ at $r = r_s$

$$D\frac{dc}{dr}|_{r=r_s} = Dc^*(\frac{1}{\sqrt{\pi Dt}} + \frac{1}{r_s}) \tag{17}$$

2.2 Hindered diffusion steady-state case

Substitution of the function into the diffusion equation, in radial coordinates yields:

$$\frac{\partial c}{\partial t} = \nabla\cdot(D(r)\nabla c) = D_0 e^{-Br_s/r}\frac{\partial^2 c}{\partial r^2} + D_0 e^{-Br_s/r}\left(\frac{2}{r} + \frac{Br_s}{r^2}\right)\frac{\partial c}{\partial r} \tag{18}$$

We can simplify this expression by limiting our analysis to the steady-state of the system:

$$0 = \frac{\partial^2 c}{\partial r^2} + \left(\frac{2}{r} + \frac{Br_s}{r^2}\right)\frac{\partial c}{\partial r} \tag{19}$$

By reducing order and substituting the boundary condition $c(x = 0, t) = 0$ and $c(x = \infty, t) = c^*$, the homogeneous ordinary differential equation directly solves to:

$$c = \frac{c^*}{e^{Br_s/r} - 1}\left(1 - e^{Br_s/r}\right) + c^* \tag{20}$$

and the steady state flux at the sphere to:

$$J_{ss} = -D_{trial}(r)\frac{\partial c}{\partial r}\bigg|_{r=r_s} = \frac{D_0 c^*}{r_s}\left[\frac{B}{(1 - e^B)}\right] \tag{21}$$

3 Anisotropic hindered diffusion towards a disc:

In cylindrical coordinates, the hindered diffusion is represented only by the normal stresses for the coordinates r and z. The gradient of the scalar field of concentration in the anisotropic diffusion equation gives the vector:

$$\frac{\partial c}{\partial t} = \nabla\cdot\{D(\frac{\partial c}{\partial r}\hat{r} + \frac{1}{\phi}\frac{\partial A}{\partial \phi}\hat{\phi} + \frac{\partial c}{\partial z}\hat{z})\} \tag{22}$$

and the diffusion coefficient is represented by a second rank tensor:

$$D = D_0\begin{bmatrix}\sigma_{rr} & \sigma_{r\phi} & \sigma_{rz}\\ \sigma_{\phi r} & \sigma_{\phi\phi} & \sigma_{\phi z}\\ \sigma_{zr} & \sigma_{z\phi} & \sigma_{zz}\end{bmatrix} \tag{23}$$

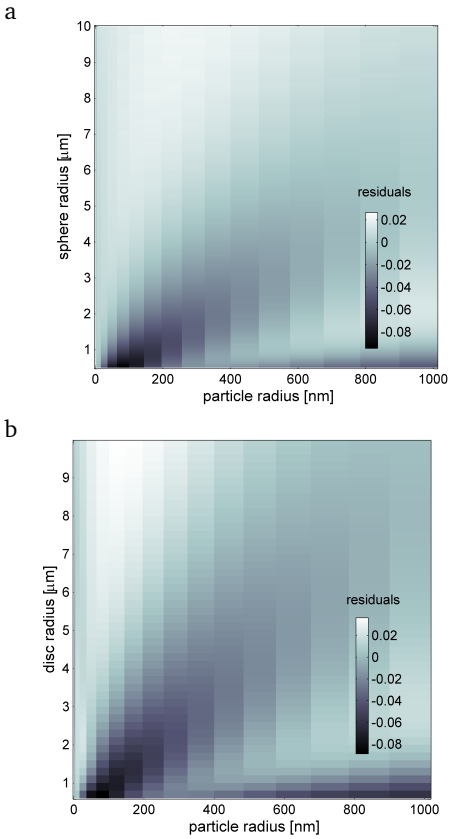

Fig. 1 The residuals map (Er) of the fitted function for the sphere (a) and the disc (b) cases, $J_{ss}(fit) - J_{ss}(simulation)$.

Recall the divergence of a vector field (A) in cylindrical coordinates:

$$\nabla \cdot A = \left(\frac{1}{r} \frac{\partial (r \cdot A_r)}{\partial r} + \frac{1}{r} \frac{\partial A_\phi}{\partial \phi} + \frac{\partial A_z}{\partial z} \right) \tag{24}$$

In axial symmetry $\frac{\partial A}{\partial \phi} = 0$. By combining the above equations we get:

$$\frac{\partial c}{\partial t} = D_0 \left(\frac{1}{r} [r \sigma_{rr} \frac{\partial^2 c}{\partial r^2} + \frac{\partial c}{\partial r} (\sigma_{rr} + r \frac{\partial \sigma_{rr}}{\partial r})] + \sigma_{zz} \frac{\partial^2 c}{\partial z^2} + \frac{\partial \sigma_{zz}}{\partial z} \frac{\partial c}{\partial z} \right) \tag{25}$$

$$\frac{\partial c}{\partial t} = D_0 \left(\sigma_{rr} \frac{\partial^2 c}{\partial r^2} + \frac{\sigma_{rr}}{r} \frac{\partial c}{\partial r} + \frac{\partial c}{\partial r} \frac{\partial \sigma_{rr}}{\partial r} + \sigma_{zz} \frac{\partial^2 c}{\partial z^2} + \frac{\partial \sigma_{zz}}{\partial z} \frac{\partial c}{\partial z} \right) \tag{26}$$

The $D \perp$ and $D \parallel$ are functions of the distance z from the electrode, or the wall adjacent to the electrode (at z=0). Therefore, $\partial \sigma_{rr} / \partial r = 0$ and the diffusion problem becomes:

$$\frac{\partial c}{\partial t} = D_0 \left(\sigma_{rr} \frac{\partial^2 c}{\partial r^2} + \frac{\sigma_{rr}}{r} \frac{\partial c}{\partial r} + \sigma_{zz} \frac{\partial^2 c}{\partial z^2} + \frac{\partial \sigma_{zz}}{\partial z} \frac{\partial c}{\partial z} \right) \tag{27}$$

4 Residual maps of the flux towards a sphere and a disc

We discuss here the result of the fitting, and we provide the residual maps for further accuracy of the flux estimation that can be used along with the approximated functions. We showed in the paper the approximate steady state functions in the case of particles impacting a sphere and a disc:

$$sphere: J^{fit}_{ss,D(r)} = 4 D_0 \pi c^* r_s (0.57 \mathrm{e}^{-2.34 \frac{r_p}{r_s}} + 0.43 \mathrm{e}^{-0.21 \frac{r_p}{r_s}} \pm Er) \tag{28}$$

$$disc: J^{fit}_{ss,D(r)} = 4 D_0 c^* r_d (0.57 \mathrm{e}^{-3.37 \frac{r_p}{r_s}} + 0.43 \mathrm{e}^{-0.26 \frac{r_p}{r_s}} \pm Er) \tag{29}$$

The functions, with an r-square value of 0.996 for sphere and 0.943 for disc, also were used as a method to find global convergence of the spatial mesh for the numerical solution as discussed in the computational methods. The local goodness of the fitting is shown by the residual map (Er) ($Er = J_{ss}(fit) - J_{ss}(simulation)$) in figure 1a for the sphere and in figure 1b for the disc. The functions provide a good fitting in most ratios of r_p/r_s, within a value of ± 0.08. The fit shows that at small targets and small particles the deviation of the simulated flux from the fitted function is relatively large $J_{ss}(fit) - J_{ss}(simulation) \sim -0.08$ which underestimates the flux. This deviation is found to be partly due to the tunnelling distance which becomes important for very small particles and targets; For very small targets the diffusion layer thickness becomes comparable to the tunnelling distance, thus small particles are being consumed before they loose a significant fraction of their hydrodynamic mobility, and a deviation from the behaviour of the exponential decay is observed. It is found that increasing artificially the β value in the tunnelling function (P) by an order of magnitude results in a maximum residual of ± 0.05.

The functions along with the residual map can also be used directly by experimentalist for the prediction of the hindered diffusion effect on the flux of particles and for an estimation of the number of impacts.

References

1 L. K. Bieniasz, O. Østerby and D. Britz, *Computers & Chemistry*, 1995, **19**, 121 – 136.

2 R. G. Compton, E. Laborda and K. R. Ward, *Understanding Voltammetry - Simulation of Electrode Processes*, Imperial College Press, 2013, p. 175.

3 S. Eloul and R. G. Compton, *J. Electroanal. Chem.*, 2016, **771**, 50 – 55.

4 E. Kätelhön and R. G. Compton, *Analyst*, 2015, **140**, 2592–2598.